University of Massachusetts Medical School

eScholarship@UMMS

2006-07-01

Role of invariant Thr80 in human immunodeficiency virus type 1 protease structure, function, and viral infectivity

Jennifer E. Foulkes-Murzycki
University of Massachusetts Medical School

Et al.

Let us know how access to this document benefits you.

Follow this and additional works at: https://escholarship.umassmed.edu/oapubs

Part of the Life Sciences Commons, and the Medicine and Health Sciences Commons

Repository Citation

Vol. 80, No. 14

Role of Invariant Thr80 in Human Immunodeficiency Virus Type 1 Protease Structure, Function, and Viral Infectivity

Jennifer E. Foulkes,[1] Moses Prabu-Jeyabalan,[1] Deyna Cooper,[1] Gavin J. Henderson,[2,3] Janera Harris,[2] Ronald Swanstrom,[2] and Celia A. Schiffer[1]*

Department of Biochemistry and Molecular Pharmacology, University of Massachusetts Medical School, Worcester, Massachusetts 01605,[1] and UNC Center for AIDS Research[2] and Department of Microbiology and Immunology,[3] University of North Carolina at Chapel Hill, Chapel Hill, North Carolina 27599-7295

Sequence variability associated with human immunodeficiency virus type 1 (HIV-1) is useful for inferring structural and/or functional constraints at specific residues within the viral protease. Positions that are invariant even in the presence of drug selection define critically important residues for protease function. While the importance of conserved active-site residues is easily understood, the role of other invariant residues is not. This work focuses on invariant Thr80 at the apex of the P1 loop of HIV-1, HIV-2, and simian immunodeficiency virus protease. In a previous study, we postulated, on the basis of a molecular dynamics simulation of the unliganded protease, that Thr80 may play a role in the mobility of the flaps of protease. In the present study, both experimental and computational methods were used to study the role of Thr80 in HIV protease. Three protease variants (T80V, T80N, and T80S) were examined for changes in structure, dynamics, enzymatic activity, affinity for protease inhibitors, and viral infectivity. While all three variants were structurally similar to the wild type, only T80S was functionally similar. Both T80V and T80N had decreased the affinity for saquinavir. T80V significantly decreased the ability of the enzyme to cleave a peptide substrate but maintained infectivity, while T80N abolished both activity and viral infectivity. Additionally, T80N decreased the conformational flexibility of the flap region, as observed by simulations of molecular dynamics. Taken together, these data indicate that HIV-1 protease functions best when residue 80 is a small polar residue and that mutations to other amino acids significantly impair enzyme function, possibly by affecting the flexibility of the flap domain.

Human immunodeficiency virus type 1 (HIV-1) protease is an enzyme crucial to the life cycle of the virus (28). Inhibition of the protease prevents viral maturation, and thus further infection, making it a prime target in the treatment of HIV-1-infected patients (8, 18, 53). Unfortunately, HIV-1 mutates frequently because of the high replication rate of the virus (9) and the infidelity of the reverse transcriptase (21, 50, 51). The viral protease tolerates mutations in many areas of the sequence, especially mutations that decrease the binding affinity of inhibitors without affecting the ability of the protease to recognize and cleave its nine processing sites within the Gag and Gag-Pro-Pol polyproteins. Such mutations cause drug resistance. Many studies have explored residues susceptible to mutation and their role in the development of drug resistance (2, 14, 23, 24, 39, 41, 55). However, some amino acids in the protease have not been observed to mutate, even in the presence of inhibitor therapy (58) (Fig. 1). While these conserved residues potentially play a crucial role in either the structure or the function of the enzyme, few studies have explored the purpose of the invariant amino acids outside the active site. Utilizing these residues could assist in the design of new classes of protease inhibitors that may be less susceptible to developing resistance.

HIV protease, a homodimeric aspartyl protease, envelops its substrate when the flap region of each monomer closes down on the substrate sites within the Gag and Gag-Pro-Pol polyproteins. In a 10-ns molecular dynamics simulation (MD) of the unliganded protease, the tips of the flaps (residues 47 to 53) were observed to curl toward the protease core like fingers curling toward the palm of a hand (57) (Fig. 1b). When the tip of the flap curls inward, Ile50 contacts a number of predominantly hydrophobic residues in its own P1 loop (residues 78 to 83). The only polar residue in this region is virtually invariant Thr80. Thr80 is one of only 27 (out of 99) residues that are invariant in 99.9% of the sequences in the Stanford University HIV Drug Resistance Database (58). The remaining 26 invariant residues include the catalytic Asp-Thr-Gly triad, five other glycines, three prolines, both tryptophans, and the tyrosine. Of the 536 HIV-1, HIV-2, and simian immunodeficiency virus protease sequences found in the Los Alamos National Laboratory Database, residue 80 is 1 of only 10 residues invariant in 99.8% of the population. Additionally, numerous crystal structures show that the side chain hydroxyl group forms highly conserved hydrogen bonds with the backbone of residue 82. Other studies have observed structural changes in the P1 loop when binding inhibitors and drug resistance mutations at Val82 and Ile84 (1, 3, 17, 25–27, 37, 48). By examining invariant residues within this loop, we may discover new ways to target protease inhibitor therapy. Interactions between Thr80 and Ile50 could be important for destabilizing the burial of Ile50 in a hydrophobic pocket and maintaining the mobility of the flap tips. Thr80 could be important for stabilizing the P1 loop through its highly conserved hydrogen bond with Val82. While the role of this residue has not been previously studied,

* Corresponding author. Mailing address: Department of Biochemistry and Molecular Pharmacology, University of Massachusetts Medical School, 364 Plantation Street, Worcester, MA 01605. Phone: (508) 856-8008. Fax: (508) 856-6464. E-mail: Celia.Schiffer@umassmed.edu.
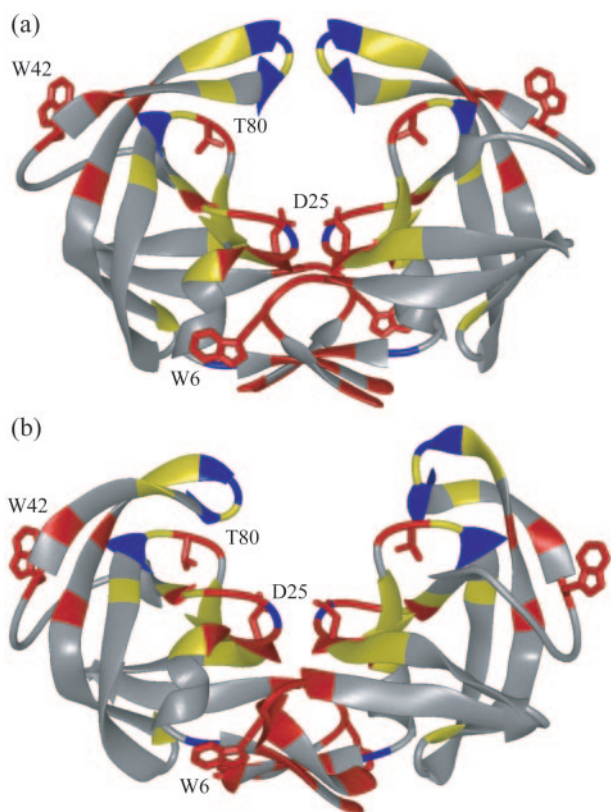
FIG. 1. HIV-1 protease colored by sequence conservation (58). Residues colored red are invariant in both untreated and treated populations of patients. Those colored yellow are invariant only in the untreated population. Invariant glycine residues are colored blue. The side chains of the catalytic aspartic acids (Asp25), Trp6, Trp42, and Thr80 are displayed. (a) Unliganded protease structure (PDB code 1HHP). (b) Protease structure following 9-ns MD simulation.

the observation that Thr80 is invariant indicates that it is likely important to protease structure and/or function.

In the present study, we used various methods to study the role of Thr80. Native Thr80 was mutated to asparagine, serine, and valine to generate protease variants referred to as T80N, T80S, and T80V. The impact of Thr80 on HIV-1 protease structure and function was investigated by a variety of biophysical methods, including circular-dichroism (CD) spectroscopy, tryptophan fluorescence, protein crystallography, MD simulations, fluorescence resonance energy transfer, and isothermal titration calorimetry. Additionally, the impact of these mutations on the virus was examined by using a virus specific-infectivity (SpIn) assay. Taken together, these data indicate that Thr80 plays an important role in enzyme activity and help to clarify why Thr80 does not mutate in vivo.

MATERIALS AND METHODS

Protease gene construction. The synthetic gene for the wild-type (WT) HIV-1 protease sequence was made with codons optimized for protein expression in *Escherichia coli* and included a substitution of Gln7Lys to prevent autoproteolysis (54). Residue 80 was mutated from threonine to three different amino acids, asparagine, serine, and valine. Mutagenesis was performed with the Stratagene QuikChange site-directed mutagenesis kit and confirmed by sequencing.

Protease expression and purification. The expression and purification of the HIV-1 protease were previously described (26, 46). Briefly, the HIV protease

gene was cloned into plasmid pXC-35 (American Type Culture Collection, Manassas, Va.) (7), which was transfected into *E. coli* TAP106. Transfected cells were grown in a 12-liter fermentor and, following protein expression, lysed to release the inclusion bodies containing the protease (20). Inclusion bodies were isolated by centrifugation, and the pellet was dissolved in 50% acetic acid to extract protease. High-molecular-weight proteins were separated from the desired protease by size exclusion chromatography on a 2.1-liter Sephadex G-75 superfine (Sigma Chemical) column equilibrated with 50% acetic acid. Refolding was accomplished by rapidly diluting the protease solution into a 100-fold excess of refolding buffer. Excess acetic acid was removed through dialysis. Protein used for crystallization was further purified with a Pharmacia Superdex 75 fast-performance liquid chromatography column equilibrated with refolding buffer.

Far-UV CD spectroscopy. To determine the effects of mutations on the secondary structure of the protease, far-UV CD spectra were measured for the WT and variant proteases with a JASCO J-810 spectrometer. The temperature was maintained at 20°C with a Peltier temperature control device. Measurements were made in a rectangular cell with a 1-mm path length. Each spectrum was obtained by averaging three spectra recorded from 250 to 200 nm at a 0.5-nm data pitch and a rate of 20 nm min^{-1}. The response time for each point was 8 s, and the bandwidth was 2.5 nm. Protease concentrations were between 5 and 11 μM in a buffer containing 10 mM sodium acetate at pH 5 and 2 mM Tris(2-carboxyethyl)phosphine. Buffer scans were subtracted from the sample scans. The mean residue ellipticity (MRE), in millidegrees per square centimeter per decimole, was calculated with the equation MRE = $\theta/(10N \times C \times l)$, where θ is the measured signal in millidegrees, N is the number of residues, C is the molar concentration of the protein, and l is the path length of the cuvette.

Tryptophan fluorescence. To further explore structural changes caused by mutations at residue 80, tryptophan fluorescence was measured in the presence and absence of saquinavir (SQV). Fluorescence was measured with a Photon Technology International spectrofluorimeter at 25°C. The excitation wavelength was 295 nm, and the emission spectrum was scanned from 300 to 500 nm in 1-nm steps. Protease concentrations were between 5 and 5.5 μM in a buffer containing 10 mM sodium acetate and 2 mM Tris(2-carboxyethyl)phosphine at pH 5. Buffer scans were subtracted from the sample scans. Each variant was also examined for changes in fluorescence upon inhibitor binding. Protease solutions were equilibrated with 30 μM SQV prior to measurement. Buffer scans containing SQV were subtracted from the sample scans.

Protein crystallization. To look for more localized changes in the structures of the proteases, T80N and T80S were crystallized with SQV, yielding the structures SQV$_{T80N}$ and SQV$_{T80S}$. Protein solutions between 1.16 and 1.75 mg ml^{-1} were equilibrated with a fivefold molar excess of the inhibitor SQV. Crystals were grown by the vapor diffusion hanging-drop method. The reservoir solution contained 126 mM sodium phosphate (pH 6.2), 63 mM sodium citrate, and 23 to 24% ammonium sulfate (25). The crystallization screens yielded rectangular crystals, with the longest dimension being 0.1 mm.

Crystallographic data collection. The crystals were mounted within 0.2-mm Hampton cryoloops and flash frozen over a nitrogen stream. Data were collected on an in-house Rigaku X-ray generator with a Raxis IV image plate. Two hundred fifty frames of 5-min exposures were collected per crystal with an angular separation of 1° and no overlap between frames. Frames containing unprocessed raw data were indexed with Denzo and scaled with ScalePack (35, 43). The SQV$_{T80N}$ and SQV$_{T80S}$ crystals diffracted to 1.5 Å and 2.0 Å, respectively. Complete data collection statistics are listed in Table 1.

Structure solution and crystallographic refinement. The crystal structures were solved and refined with the programs within the CCP4 interface (10). The structures of SQV$_{T80N}$ and SQV$_{T80S}$ were solved with the molecular replacement program AMoRe (40). The coordinates of the WT protease in complex with the substrate (Protein Data Bank [PDB] code 1F7A) (47) were used as the starting model. Upon obtaining the rotation and translation solutions, the molecular replacement phases were further improved by using ARP/wARP (36) to build solvent molecules into the unaccounted for regions of electron density. Subsequently, interactive model building was carried out with O (22). Initial 2Fo-Fc and Fo-Fc maps unambiguously yielded the positions of SQV in each complex. Conjugate gradient refinement with Refmac5 (38) was performed by incorporating the Schomaker and Trueblood tensor formulation of translation, libration, and screw rotation parameters (30, 56, 61). The working R (R$_{work}$) and its cross validation (R$_{free}$) were monitored throughout refinement. The geometry of the structure was assessed with Procheck (31) at the end of each refinement round. The refinement statistics are also shown in Table 1.

Isothermal titration calorimetry. To assess changes in the interaction between each variant and SQV relative to that of the WT, the binding affinity and enthalpy of interaction between each protease variant and SQV were measured by competitive displacement isothermal titration calorimetry experiment (26, 42,

TABLE 1. Crystallographic statistics of variant HIV-1 proteases T80S and T80N in complex with SQV[a]

Parameter	SQV$_{T80S}$	SQV$_{T80N}$
Data collection		
Space group	P2$_1$2$_1$2$_1$	P2$_1$2$_1$2$_1$
Z	4	4
a (Å)	50.50	50.52
b (Å)	57.93	58.18
c (Å)	61.62	61.52
Resolution (Å)	2.0	1.5
Total no. of reflections	88,158	123,033
No. of unique reflections	12,625	29,647
R$_{merge}$ (%)	7.3	4.2
Completeness (%)	99.1	99.3
I/σ$_I$	8.2	17.7
Refinement		
R$_{work}$ value (%)	17.6	17.1
R$_{free}$ (%)	23.2	19.8
R$_{work}$ + R$_{free}$ (%)	17.9	17.3
RMSD		
Bond length (Å)	0.008	0.005
Bond angle (°)	1.6	1.4
No. of waters	130	193
No. of phosphates	5	6
PDB code	1FGU	1FGV

[a] RMSD, root mean square deviation.

60, 62, 64) on a VP isothermal titration calorimeter (MicroCal Inc., Northampton, MA). The buffer used for all protease and inhibitor solutions consisted of 10 mM sodium acetate (pH 5.0), 2.0% dimethyl sulfoxide, and 2 mM Tris(2-carboxyethyl) phosphine. A 25 to 30 μM protease solution was saturated with 29 10-μl injections of 0.3 mM pepstatin. The pepstatin was then displaced from the protease by adding 29 10-μl injections of 0.25 mM SQV. Heats of dilution were subtracted from the corresponding heats of reaction to obtain the heat due solely to binding of the ligand to the enzyme. The binding affinity and enthalpy of the interaction between the protease and SQV were obtained by using the Origin7 software to subtract the enthalpy and binding affinity of pepstatin from the final displacement reaction. Direct SQV titration experiments were performed for T80N because this variant did not bind pepstatin and the direct titration of SQV versus this variant yielded high-quality results. Twenty-nine 10-μl aliquots of 0.2 mM SQV were injected into solutions containing 22 to 40 μM protease. Data were processed and analyzed with the MicroCal Origin7 software package. Final results represent the average of three measurements.

Enzymatic activity. Changes in the catalytic activity of each protease variant were assessed by measuring each variant's ability to hydrolyze the fluorogenic substrate Arg-Glu(EDANS)-Ser-Gln-Asn-Tyr-Pro-Ile-Val-Gln-Lys(DABCYL)-Arg (Molecular Probes, Eugene, OR) (34). Fluorescence reactions were monitored by exciting solutions at 340 nm and recording emitted light at 490 nm in a Photon Technology International spectrofluorimeter. Substrate solution (190 μl) was placed in a 3-mm rectangular cuvette, and baseline fluorescence was measured. The reaction was initiated by adding 10 μl of 2 μM HIV-1 protease solution. After 20 s (the time needed for manual mixing), data points were acquired every 2 s. At substrate concentrations above 10 μM, results were tainted by the inner-filter effect (11). The fluorogenic substrate was dissolved in 1 M sodium chloride–0.1 M sodium acetate–1 mM EDTA–1 mM dithiothreitol–4% dimethyl sulfoxide–1 mg/ml bovine serum albumin at pH 4.7, and the experiments were done at 25°C. The baseline fluorescence of the substrate solution was subtracted from the reaction fluorescence. The increase in fluorescence was monitored in real time, and when there was no further increase in fluorescence the reaction was considered complete. Initial data analysis showed that the K_m was above 10 μM and K_m and k$_{cat}$ could not be separately determined. Therefore, k$_{cat}$/K_m was determined with substrate concentrations below K_m (11). The increase in fluorescence over time was fitted by Kaleidagraph (v 3.6) to the equation $y = m_1 + m_2 \times (1 - e^{(-m_3 \times x)})$, where m_1 is the initial fluorescence, m_2 is the total increase in fluorescence, and m_3 is [E] × k$_{cat}$/K_m. For each

protease variant that reacted with the fluorescent substrate, k$_{cat}$/K_m was calculated at concentrations of 2, 5, and 10 μM substrate. The average k$_{cat}$/K_m was calculated over nine values, three at each substrate concentration.

SpIn assay. The SpIn assay was performed as described by G. J. Henderson et al. (unpublished data). Mutations were introduced into the protease region of a plasmid subclone of the NL4-3 strain of HIV-1 by the QuikChange strategy. The mutagenized subclone was verified completely by sequence and then introduced into a full-length clone of NL4-3 called pNL-CH. Two clones of each mutant were isolated, and the protease nucleotide sequence was confirmed. The mutagenized plasmids were used to generate infectious virus by transfecting 293 cells that were plated at a density 3 × 10^5 per well of a 24-well plate 1 day prior to transfection. Triplicate transfections of 0.5 μg of each plasmid DNA were done with each mutant plasmid with Fugene transfection reagent (Roche) according to the manufacturer's instructions. The parental WT plasmid was transfected in parallel, also in triplicate, for direct comparison with the mutants. After 48 h, virus-containing culture supernatants were collected, clarified of cellular debris by centrifugation at 3,000 × g and 4°C for 5 min, and then stored at −80°C. The amount of capsid protein (p24) in the culture supernatants was measured by an enzyme-linked immunosorbent assay with reagents available from the National Cancer Institute AIDS Vaccine Program. The manufacturer's instructions were followed, except that samples were mixed with sodium dodecyl sulfate (final concentration, 1% [wt/vol]) and incubated at 100°C for 5 min for virion lysis. All samples were measured in duplicate at two dilutions, and the masses were calculated from the standard curve by using the average optical density of the duplicate measurements. Virus particles were also analyzed by Western analysis as described previously (49), with a polyclonal anti-p24 antibody (NIH AIDS Research and Reference Reagent Program, 4250). Briefly, virus particles in the medium supernatant of transfected cultures were collected by centrifugation and lysed. The lysed viral proteins were resolved by polyacrylamide gel electrophoresis under denaturing and reducing conditions, and the proteins were then transferred to a membrane and probed with an anti-p24 antibody.

The infectivity of the mutant viruses was measured by infecting TZM-bl cells (AIDS Research and Reference Reagent Program, National Institutes of Health) that were seeded at 1.3 × 10^4 cells per well of a 96-well plate 24 h prior to infection. After a 48-h incubation with the virus, the cells were washed with 150 μl of Dulbecco's phosphate-buffered saline, lysed with 50 μl of luciferase reporter lysis buffer (Promega), and stored at −80°C. The samples were subsequently thawed. The amount of luciferase activity present was quantified over a 4-s interval when 50 μl of luciferase reagent (Promega) was injected in each well with a FLUOstar fluorescence plate reader (BMG LABTECH) to record the number of relative light units emitted. SpIn, calculated as the number of relative light units per nanogram of infecting capsid protein, was normalized to the parental strain, which was given a SpIn value of 1.

MD. To study the impact of mutating residue 80 on the conformational flexibility of HIV-1 protease, separate MD simulations were run for the WT and three protease variants, T80S, T80N, and T80V. The initial coordinates were taken from the 9-ns time point of a previous simulation where the protease flap tips were already folded in toward the P1 loop (57). Each mutation (serine, asparagine, or valine) was modeled by MIDAS (16) into residue 80 in both monomers, and MD simulations were started with the AMBER8 software package (6). Histidine residues were protonated at the epsilon nitrogen. Two hundred cycles of restrained steepest-descent energy minimization were performed on each structure. The protein was restrained with a harmonic force constant of 9.55 kcal mol^{-1} Å^{-2}. Each structure was solvated with a TIP3P water box to allow for at least 8 Å of water on each face of protease. The initial periodic box dimensions were 82.2 by 82.6 by 80.4 Å^3. Approximately 14,000 water molecules were added to each system, and 1,000 cycles of steepest-descent energy minimization were performed, keeping the protein fixed. Equilibration of the system continued with 5,000 steps of restrained MD with a 9.55-kcal mol^{-1} Å^{-2} force constant and constant temperature (300 K) and pressure (1 atm). This equilibration was followed by 25,000 steps of unrestrained MD. The data-collecting portion of the simulation was performed at constant temperature and pressure for 5 ns with 1-fs time steps.

RESULTS

The role of residue 80 in the structure, function, and viral infectivity of the HIV-1 protease was investigated in three variants, T80N, T80V, and T80S.
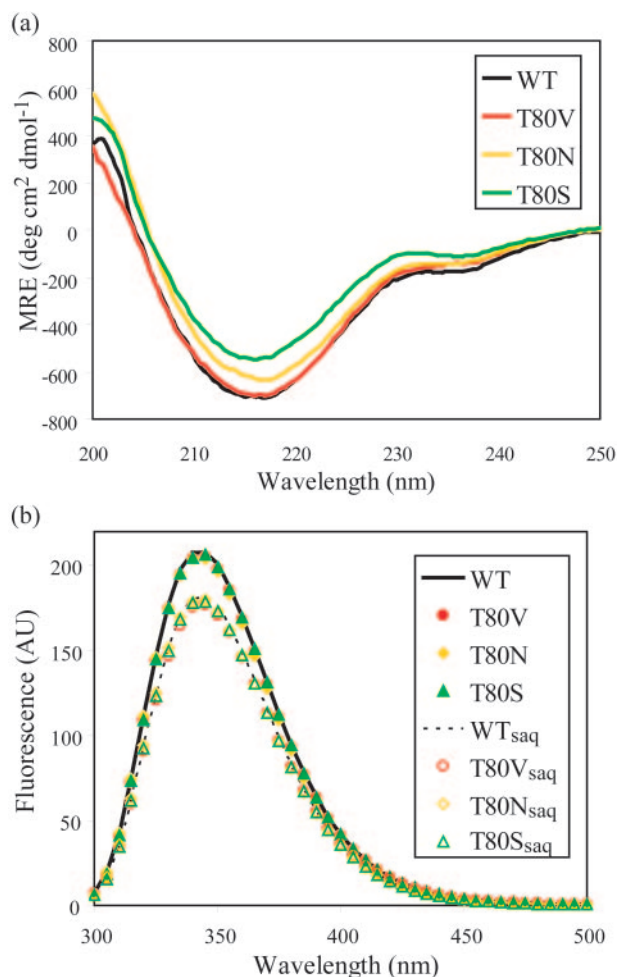
FIG. 2. General structural features of WT and variant proteases (WT, black; T80V, red; T80N, yellow; T80S, green). (a) Far-UV CD spectra of WT and variant proteases. (b) Tryptophan fluorescence spectra of WT and variant proteases, unbound and bound to SQV. The unliganded WT protease is shown as a solid line, and the unliganded variant proteases are shown as filled symbols. The WT protease bound to SQV is shown as a dotted line, and the variant proteases are shown as empty symbols. AU, arbitrary units.

General structural changes. Effects of the three mutations on the secondary structure of the HIV-1 protease were probed by far-UV CD spectroscopy. Since HIV-1 protease is a predominantly β-sheet protein, any mutation that dramatically disrupted the structure would decrease the β-sheet content of the protein and increase its MRE at 216 nm. As shown in Fig. 2a, the three variants had secondary structures similar to that of the WT, comparable to previously published results (65).

The spectrum of T80V was almost identical to that of the WT protease, and within the accuracy of protein concentration measurements, those of T80S and T80N were similar to that of the WT. The overall resemblance among these spectra indicates that these proteases were all folded similarly.

To further examine any structural changes caused by mutations at residue 80, tryptophan fluorescence was measured for all variants. Each protease monomer has two tryptophans, Trp6 at the dimer interface and Trp42 at the end of the flap region (Fig. 1). The fluorescence of the native tryptophans was measured for the WT protease and each variant in the presence and absence of SQV. The emission spectra for T80V, T80S, and T80N were similar to that of the WT, indicating that the tryptophans in the Thr80 protease variants are in an environment similar to that of those in the WT protease (Fig. 2b). For both the WT and variant proteases, the presence of SQV led to a 10% decrease in the observed tryptophan fluorescence, suggesting that SQV interacts with all of these proteases. However, these results did not provide information on how this interaction may have been altered by mutation at Thr80.

Thermodynamic parameters of inhibitor binding. To reveal any altered interactions between SQV and the Thr80 variant proteases, the binding affinity and thermodynamic parameters of each variant and WT with respect to SQV were determined by isothermal titration calorimetry (Table 2). SQV was chosen because it is a well-characterized protease inhibitor (12, 15, 19, 29, 33, 52, 64). SQV is an entropically driven inhibitor. As SQV is a fairly hydrophobic molecule, it likely causes surrounding water molecules to become ordered. The favorable entropy observed in the reaction between the HIV-1 protease and SQV is presumably due to the release of this ordered water when SQV is sequestered within the active site of the protease. The free energy of binding of T80N and SQV was 4.2 kcal mol^{-1} worse than that between the WT and SQV. This decreased binding affinity was associated with larger changes in the enthalpy and entropy of the reaction. The entropy of T80N binding to SQV was 13.4 kcal mol^{-1} more favorable than that of the WT, while the enthalpic contribution was 17.7 kcal mol^{-1} less favorable. Similarly, a small decrease in binding affinity between T80V and SQV was associated with larger changes in the enthalpy and entropy of the reaction. While the free energy of the reaction between T80V and SQV decreased by 0.5 kcal mol^{-1} relative to that of the WT, the entropy of SQV binding was 4.5 kcal mol^{-1} more favorable and the enthalpy of the reaction was 5.0 kcal mol^{-1} less favorable than its binding to the WT. In contrast to the other two variants, there was no change within error in the free energy of the reaction between T80S and SQV relative to that of the WT. While the entropy of T80S binding to SQV was 0.5 kcal mol^{-1} more favorable than that of WT binding to SQV, the free energy of the reac-

TABLE 2. Binding thermodynamics of SQV at 20°C

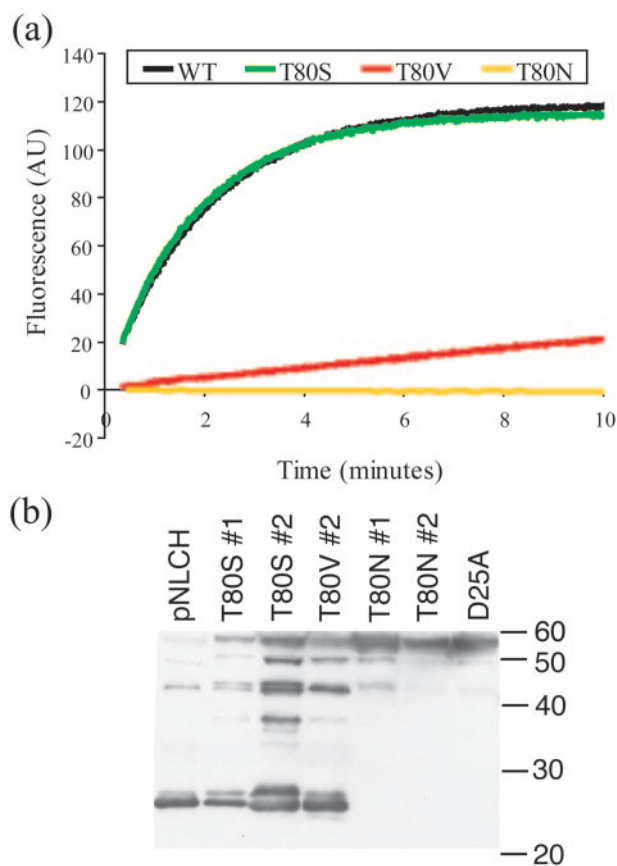| Protease	K_a (M^{-1})	K_d (nM)	K_d ratio	ΔH (kcal mol^{-1})	$\Delta\Delta H$	$-T\Delta S$ (kcal mol^{-1})	$\Delta(-T\Delta S)$	ΔG (kcal mol^{-1})	$\Delta\Delta G$
WT	$(2.0 \pm 0.1) \times 10^9$	0.50 ± 0.03		3.6 ± 0.1		-16.1		-12.5	
T80S	$(1.5 \pm 0.1) \times 10^9$	0.66 ± 0.05	1.3	4.2 ± 0.3	0.6	-16.5	-0.4	-12.3	0.2
T80V	$(8.8 \pm 0.1) \times 10^8$	1.1 ± 0.02	2.3	8.6 ± 0.3	5.0	-20.6	-4.5	-12.0	0.5
T80N	$(1.3 \pm 0.1) \times 10^6$	760 ± 43	1.5×10^3	21 ± 1.7	18	-29.5	-13	-8.2	4.3

FIG. 3. Mutation at residue 80 affects protease activity. (a) Enzymatic activity. The increase in fluorescence over time observed when 10 μl of a 2 μM protease solution was mixed with 190 μl of 2 μM fluorescent substrate is shown. Both the WT (black) and T80S (green) completely cleaved the fluorescent substrate within 10 min. The initial burst in fluorescence occurs during the 20 s required for mixing. T80V (red) required 10 min to reach the same fluorescence that the WT and the T80S variant achieved in the first 20 s. The T80N (yellow) variant had virtually undetectable increases in fluorescence. AU, arbitrary units. (b) Western analysis of mutant virus particles. Lane 1, pNLCH used as the WT; lane 2, T80S mutant; lane 3, another clone of the T80S mutant; lane 4, T80V mutant; lane 5, T80N mutant; lane 6, another clone of the T80N mutant; lane 7, D25A active-site mutant of the protease used as a control for a negative processing phenotype. Molecular size markers were included in the gel, and their migration positions (sizes are in kilodaltons) are shown on the right.

tion was maintained at approximately the same value by 0.7 kcal mol^{-1} less favorable enthalpy. The thermodynamic parameters of all reactions were measured with SQV. Therefore, the changes in enthalpy and entropy were likely due exclusively to changes in the free and bound states of the enzyme between the variants. Both the Thr80Val and Thr80Asn mutations decreased the binding affinity of protease for SQV, and all three mutations affected the thermodynamics of binding between the protease and SQV, demonstrating the importance of Thr80 in the activity of the protease.

Enzymatic activity. An assay of enzymatic activity was used to further verify the importance of Thr80 to protease function. Each variant protease was examined for deleterious effects on activity relative to the WT through comparison of the ability of each variant to cleave a fluorogenic MA-CA substrate. Both

the WT and T80S completely cleaved all of the fluorescent substrate within 10 min (Fig. 3a). T80V required more than 2 h to completely cleave all of the substrate. T80N was not able to cleave the substrate. The catalytic efficiencies, k_{cat}/K_m values, of the WT and T80S were 7.4×10^{-2} μM^{-1}s^{-1} and 8.4×10^{-2} μM^{-1} s^{-1}, respectively (Table 3), indicating greater catalytic activity for the T80S variant. The k_{cat}/K_m of T80V was 4.5×10^{-3} μM^{-1}s^{-1}, a 16-fold decrease relative to that of the WT. The impact of the Thr80Val and Thr80Asn mutations on protease activity further confirms the importance of Thr80 in protease function.

Viral infectivity. A SpIn assay of viral fitness was performed with the Thr80 mutants to provide information about the proteases' abilities to cleave the substrate sites necessary for viral maturation. The measured infectiousness of both the T80S virus and the T80V virus was within twofold of that of the WT virus. The apparent discrepancy between the enzymatic activity and the SpIn was probably due to the fact that the MA-CA cleavage site is not the rate-determining step in viral maturation (32, 44, 45, 63). This indicates that, despite impaired activity versus the MA-CA site, T80V was still able to cleave other sites with sufficient efficiency to maintain nearly WT levels of infectivity. In contrast, the T80N virus had very low levels of infectivity. When we examined the extent of processing by Western analysis (Fig. 3b), we found that the T80N virus were composed of mostly unprocessed Gag, similar to a D25A protease active-site mutant virus. In contrast, the T80S virus and the T80V virus were composed of Gag that had been largely processed although to a lesser extent than the WT virus.

Structures of protease-SQV complexes. The Thr80Asn mutation consistently impaired protease activity, while the Thr80Ser mutation did not affect protease activity. To determine what structural changes were causing the observed effect on protease activity, T80N and T80S were crystallized with SQV, yielding the structures SQV$_{T80S}$ and SQV$_{T80N}$, with 2.0-Å and 1.5-Å resolutions, respectively. These structures were submitted to the PDB and assigned codes 1FGU and 1FGV, respectively. The electron density of both SQV and the mutated side chains was unambiguous, and there were no crystal contacts between the mutated side chains and surrounding protease molecules. The crystallographic statistics for these structures are listed in Table 1. The PDB structure of the WT HIV-1 protease bound to SQV (PDB code 1HXB) (29) has SQV in two orientations. In order to obtain the most accurate comparison between structures and because T80S behaved just as the WT did, the SQV$_{T80N}$ and SQV$_{T80S}$ structures were compared with each other. To look for changes between the SQV$_{T80N}$ and SQV$_{T80S}$ structures, difference distance plots with the C$_\alpha$ backbone of each structure were generated comparing the two protein variants (Fig. 4). This plot shows that one monomer of the SQV$_{T80N}$ structure underwent significant

TABLE 3. Catalytic efficiencies of WT and variant proteases

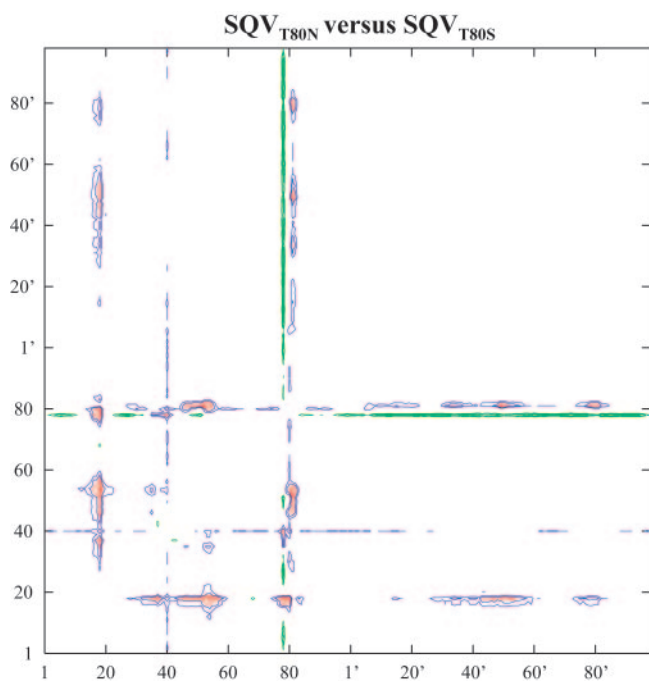| Protease	k_{cat}/K_m (μM^{-1} s^{-1})
WT	$(7.4 \pm 0.5) \times 10^{-2}$
T80S	$(8.4 \pm 1.3) \times 10^{-2}$
T80V	$(4.5 \pm 2.0) \times 10^{-3}$
T80N	No detectable activity

FIG. 4. Difference distance plots of SQV_{T80N} versus SQV_{T80S}. Relative changes in the distance between two alpha-carbon atoms in the SQV_{T80S} structure versus the SQV_{T80N} structure are shown. Green, blue, and red contours distinguish the ranges −1.0 to −0.5 Å, 0.5 to 1.0 Å, and 1 Å and above, respectively.
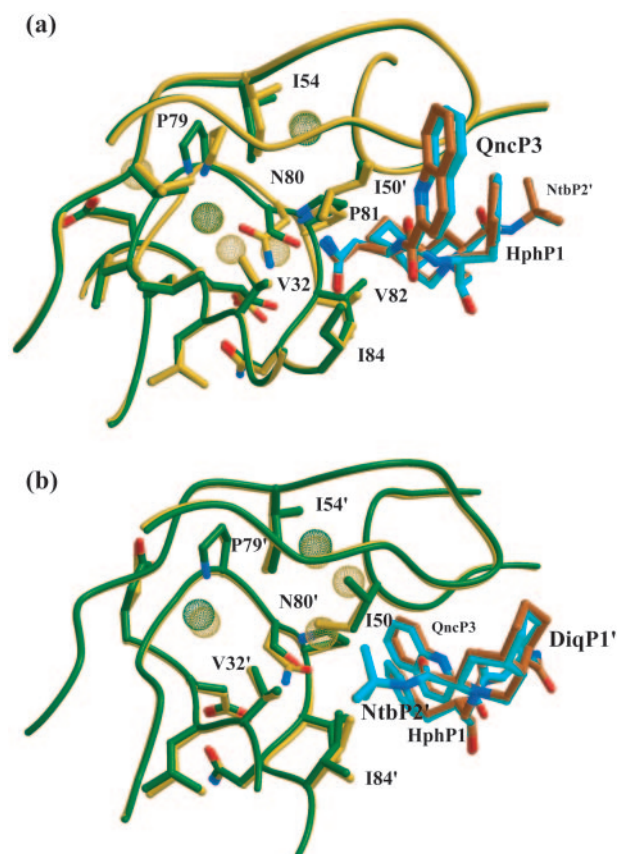

FIG. 5. P1 loops of the crystal structures of SQV_{T80N} and SQV_{T80S} superimposed. Side chain oxygen atoms are in red, and side chain nitrogen atoms are in blue. Water molecules within 5 Å of residue 80 are shown as van der Waals spheres. (a) Asn80 (SQV_{T80N}, yellow; SQV, orange) and Ser80 (SQV_{T80S}, green; SQV, cyan) adopt very different conformations in the P1 loop. (b) Asn80′ and Ser80′ adopt similar conformations, and the P1 loops in this monomer are not significantly different between the two structures. The modeling program MIDAS (16) was used to superimpose the two protease structures, SQV_{T80N} and SQV_{T80S}, on the basis of the highly conserved terminal region (positions 1 to 9 and 86 to 99).

structural rearrangement to accommodate asparagine, while the other monomer was able to accommodate the larger side chain without altering the position of the main chain atoms of the protease.

While residue 80 is not in the active site of the protease, it is bound to and contacts residues directly involved in ligand binding. Therefore, a mutation at this residue could cause significant rearrangement of the protease with inhibitor bound. As shown in the double difference distance plot, the distance between residues Pro79 through Val82 and most regions of the protein increased by more than 0.5 Å in SQV_{T80N} relative to SQV_{T80S}. The most significant increases were with residues in both flap regions, Lys43-Gln58 and Lys43′-Gln58′ and the P1 loop in the opposite monomer, Pro79′-Val82′. In SQV_{T80N}, the side chain of Asn80 folded back on itself (Fig. 5a). Relative to Ser80, this conformation of Asn80 increased its interaction with Val32 and Leu33 and formed a hydrogen bond between Asn80 OD and Pro79 N. The side chain amide nitrogen of Asn80 and the side chain carboxyl oxygen of Ser80 maintained the conserved hydrogen bond with the backbone oxygen of Val82. However, the conformation of Asn80 altered the P1 loop relative to its position in SQV_{T80S}, pulling Pro81 back from the 2-methyl-decahydroisoquinoline-3-carboxylic acid-P1′ (DiqP1′) group of SQV and Val82 toward DiqP1′. In SQV_{T80N}, SQV lost a contact with Pro81, which was above it, when the distance between Pro81 CG and DiqP1′ C5 increased by 0.7 Å and gained a contact with Val82, which was below it, when the distance between Val82 CG1 and DiqP1′ C6 decreased by 0.9 Å in SQV_{T80N} relative to SQV_{T80S}. Figure 6b shows contacts that decreased by more than 0.2 Å in

SQV_{T80N} relative to SQV_{T80S}, and the opposite information is displayed in Fig. 6a. These results emphasize that structural rearrangement of the P1 loop can significantly alter the interactions between the protease and SQV.

Although one monomer of the SQV_{T80N} structure had rearranged the P1 loop relative to SQV_{T80S}, the other monomer did not undergo any repositioning of its main chain atoms relative to the SQV_{T80S} structure. As shown in the double difference plot, the distance between 80′ C_α and other residues was not significantly different between the SQV_{T80N} and SQV_{T80S} structures, indicating that when the protease variants were bound to SQV, the protease was able to accommodate asparagine at residue 80′. Asn80′ adopted a conformation similar to that of Ser80′ (Fig. 5b), and both residues formed the same hydrogen bonds with the main chain atoms of Pro81′ and Val82′. A significant difference between the two structures was the presence of a water molecule in the SQV_{T80N} structure between Ile50 and residues Pro79′ and Pro81′ that was not observed in the SQV_{T80S} structure. This water molecule forms
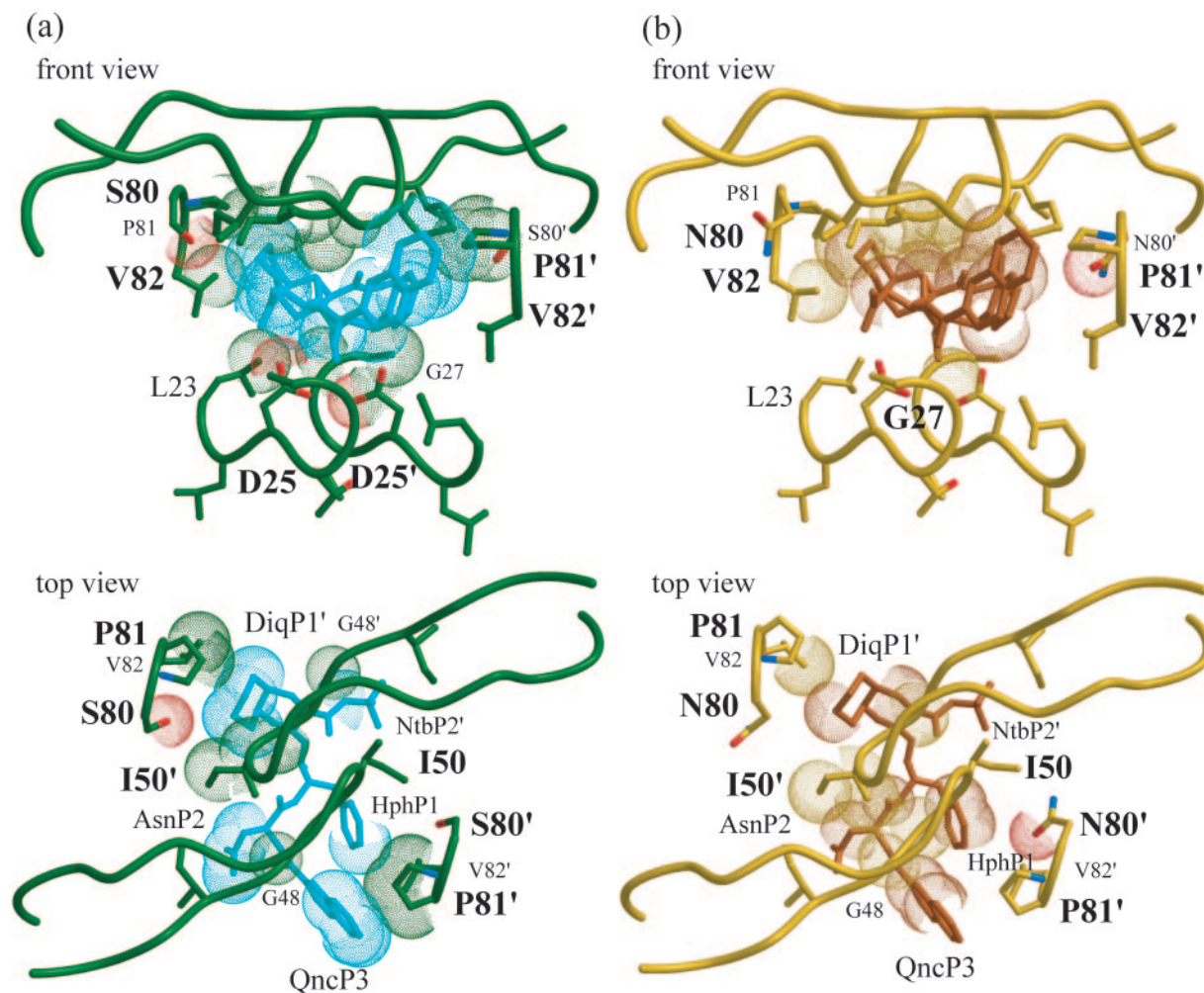
FIG. 6. Differences in van der Waals contacts between the protease and SQV in the SQV$_{T80S}$ and SQV$_{T80N}$ crystal structures. Distances between these two structures that changed by more than 0.2 Å were considered significant. Side chain oxygen atoms are in red, and side chain nitrogen atoms are in blue. (a) van der Waals spheres are used to show contacts between protease atoms and SQV atoms that decreased by more than 0.2 Å in SQV$_{T80S}$ relative to SQV$_{T80N}$. (b) van der Waals spheres are used to show contacts between protease atoms and SQV atoms that decreased by more than 0.2 Å in SQV$_{T80N}$ relative to SQV$_{T80S}$.

one hydrogen bond with the side chain amine group of Asn80′, one contact with SQV, and numerous contacts with both main chain and side chain atoms of Ile50, Pro79′, Asn80′, and Pro81′. Despite the increased size of asparagine and the presence of the extra water molecule, there was remarkable similarity of this monomer between the structures. However, there was some structural rearrangement of SQV and a few variations in the van der Waals contacts made between the protease and SQV. There was one contact between Asn80′ and the phenylalaninol-P1 group of SQV not observed in the SQV$_{T80S}$ structure. Conversely, the distance between Pro81′ and the phenylalaninol-P1 and 2-carbonylquinoline-P3 groups was increased by more than 0.2 Å in SQV$_{T80N}$ relative to SQV$_{T80S}$. Two van der Waals contacts were lost between SQV and the SQV$_{T80N}$ variant protease because of this increased distance (Fig. 6). This indicates that, in contrast to the structural rearrangements observed by residues Pro79 and Val82, the altered interactions between SQV and protease in this monomer are due to rearrangements of SQV to accommodate Asn80′.

Interactions between SQV and the protease flap region differed between SQV$_{T80N}$ and SQV$_{T80S}$. These changes were caused by the structural modifications that were made by either the P1 loops or SQV. For example, in the SQV$_{T80S}$ structure, the DiqP1′ group has the most van der Waals contacts with the flap region while in the SQV$_{T80N}$ structure, the asparagine-P2 group of SQV had the most contact with the flap region. The 2-carbonylquinoline-P3 group of SQV was closer to Gly48, and asparagine-P2 moved closer to Ile50′ in SQV$_{T80N}$ relative to their distance in SQV$_{T80S}$. Thus, substitution of asparagine at residue 80 was able to indirectly affect the flap region in the bound protease.

Changes in flap dynamics. In order to further examine the role of residue 80 in the structure and conformational flexibility of the flap region of the unbound protease, a separate MD simulation was performed for the WT and each variant protease, T80V, T80N, and T80S. Each simulation was started from the 9-ns structure of the previous MD simulation (57) since the flap region was already folded in toward the P1 loop
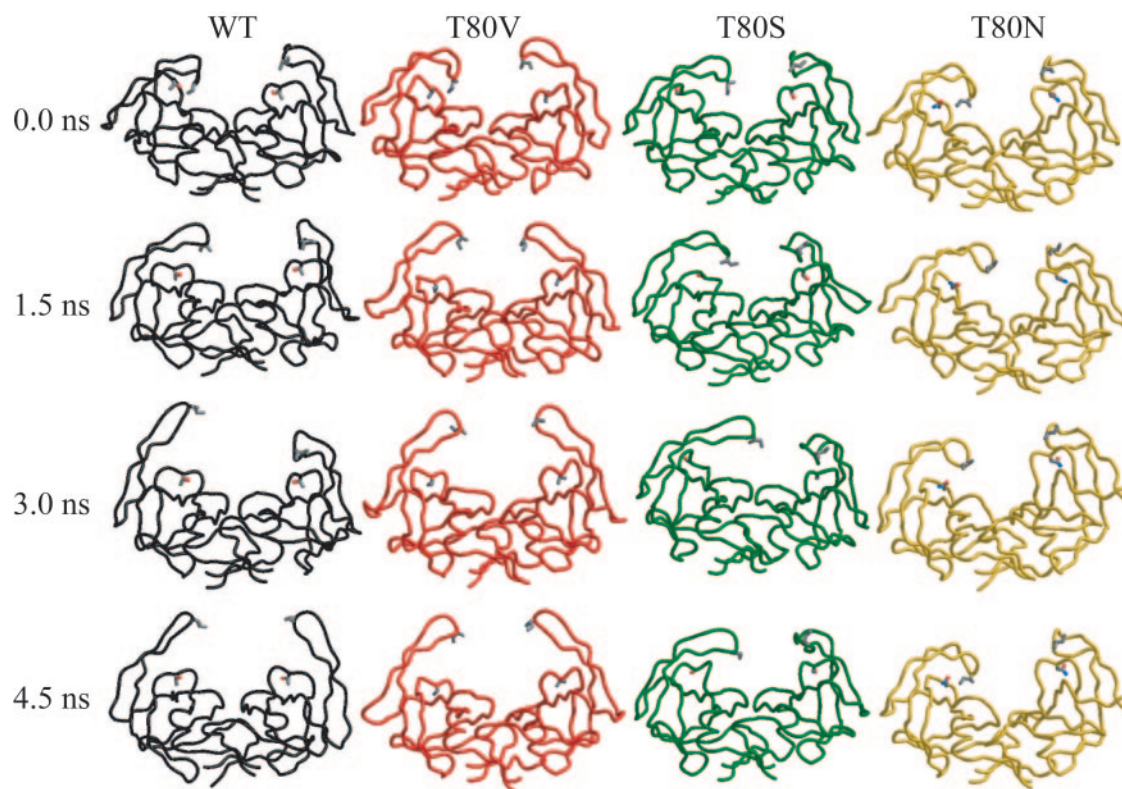
FIG. 7. Snapshots from the four MD simulations at 0.0, 1.5, 3.0, and 4.5 ns (WT, black; T80V, red; T80S, green; T80N, yellow). The flap region in the WT, T80V, and T80S simulations unfolded into the solvent within 4.5 ns. In the T80N simulations, the flap region was less mobile.

in this structure. Because these were relatively short simulations and nothing was restraining the protease, the two monomers in each simulation exhibit two conformational samplings of protease monomers. Figure 7 shows four time snapshots from the four simulations at 0 ns, 1.5 ns, 3 ns, and 4.5 ns. The WT, T80S, and T80V simulations sampled similar conformational spaces. Although each monomer moves separately, in all three simulations the protease flap region unfolds into the solvent. To quantify the range of motion of the protease flaps in each simulation, the distance between residue 50 and residue 80 in both monomers in all of the simulations was monitored over time. In the WT, T80V, and T80S simulations, the distance between these two residues fluctuated between 5 and 22 Å in both monomers. In one monomer of the T80S simulation, the space sampled by the flap region was significantly decreased, relative to the WT and its other monomer, because of a hydrogen bond between the backbone oxygen of Pro79 and the backbone nitrogen of Ile50. After approximately 3.5 ns, that hydrogen bond was broken and the flap began to unfold into the solvent. In contrast to the other simulations, the flaps within the T80N simulation did not unfold into the solvent. As shown in Fig. 7, there was decreased flexibility in both flap regions in the T80N simulation relative to the other protease variants. The distance between Asn80 and Ile50 fluctuated between 7 and 17 Å in one monomer and between 6 and 8 Å in the other monomer. In this simulation, the flap region with decreased movement was bound to the P1 loop by two hydrogen bonds, one between the side chain oxygen of Asn80 and the backbone nitrogen of Gly49 and the other between the

backbone oxygen of Pro79 and the same backbone nitrogen of Gly49. In the other monomer, there was not a specific hydrogen bond between the flap region and the P1 loop, yet this flap remained curled toward the P1 loop for most of the simulation. This was probably due to water bridging hydrogen bonds between the flap and Asn80. These results demonstrate that substituting a large polar residue for threonine at residue 80 can significantly and detrimentally affect the conformational flexibility of the flap region. However, substitution of a nonpolar residue did not impact the ability of the protease flap to unfold into the solvent.

As mentioned previously, there is a conserved hydrogen bond between the side chain of residue 80 and the backbone of residue 82. In these simulations, the existence of this hydrogen bond over time was monitored, except in the T80V simulation, where no hydrogen bond can exist. In the WT simulation, this hydrogen bond existed less than 10% of time, and in the T80S simulation it existed less than 1% of the time. It did not exist in the T80N simulation. As shown in Fig. 7, this hydrogen bond was not required to maintain the stability of the P1 loop. These simulations provide interesting insights into the impact of variation at residue 80 on protease dynamics and may help to explain the results seen in the various activity assays described above.

DISCUSSION

Many residues within the HIV-1 protease are susceptible to mutation, especially under the selective pressure of therapy;

therefore, those residues that are invariant despite therapy are likely important to enzyme structure and/or function. Thr80, which is invariant in the HIV-1, HIV-2, and simian immunodeficiency virus proteases, regardless of protease inhibitor treatment, is one such residue. While not directly involved in ligand binding, it is located on the edge of the active-site cavity in the middle of the P1 loop. To examine the role of this residue in protease, we constructed three protease variants, T80S, T80N, and T80V, and used a variety of biochemical techniques to characterize its role in the structure, dynamics, and function of protease. Additionally, a viral infectivity assay was used to examine the impact of changes at residue 80 on the virus as a whole. The results indicate that mutation at this site can detrimentally impact the enzymatic activity, decrease viral infectivity, alter the enthalpy and entropy contributions to inhibitor binding, and likely decrease the conformational flexibility of the HIV-1 protease.

Of the three variants studied, T80S had the least impact on protease structure and function. This variant had a slightly increased k_{cat}/K_m relative to the WT but no substantial change in its affinity for SQV and only an approximately twofold effect on viral infectivity. Thus, this mutation does not appear to give the virus any selective advantage or cause any resistance to SQV. Further studies are needed to clarify why Thr80Ser does not occur as a natural variant. Regardless of the amino acid at residue 80, all of the protease variants had structures similar to that of the WT (Fig. 2). Two variants, T80S and T80N, were crystallized with the inhibitor SQV. The structures were remarkably similar, except that the Thr80Asn mutation led to a structural rearrangement of the P1 loop in one monomer relative to the SQV_{T80S} structure (Fig. 5) that altered the van der Waals contacts of T80N relative to those of T80S (Fig. 6). Despite the rearrangement of this loop, the asparagine at this site was able to form hydrogen bonds with Val82. In fact, maintenance of this hydrogen bond maybe what led to the rearrangement of the P1 loop in this monomer. The hydrogen bond between the side chain of residue 80 and the backbone of Val82 was also observed in the other monomer of SQV_{T80N} and in both monomers of SQV_{T80S}. Thus, an important role of Thr80 in the bound protease appears to be the formation of this hydrogen bond.

While this hydrogen bond was conserved in the crystal structures, it was not conserved in the MD simulations of unbound protease. MD simulations were performed on all variant proteases and on the WT. In the WT, T80S, and T80N simulations, residue 80 was capable of forming a hydrogen bond between its side chain and the backbone of Val82. However, this hydrogen bond existed only intermittently in the WT and T80S simulations and did not exist in the T80N simulation. Without the hydrogen bond between residue 80 and Val82, the P1 loop itself was still structurally stable. Actually, residue 80 appeared to have the most significant impact on the flexibility of the flap region. In the WT, T80S, and T80V simulations, the flap region uncurled into the solvent (Fig. 7). This was somewhat surprising in the T80V simulation because our original hypothesis was that polar Thr80 prevented Ile50 from packing into the hydrophobic pocket formed by other residues surrounding the P1 loop. Unexpectedly, the polar asparagine at residue 80 prevented the flap from uncurling by forming electrostatic interactions with the flap region, limiting its flexibility.

While crystal structures of the bound protease would not suggest that residue 80 is involved in flap dynamics, MD simulations illustrate a potential role for this site in flap dynamics.

Although residue 80 is not in the active site of the protease, it is bound to and contacts numerous residues involved in ligand binding. Therefore, mutations at this site could have an indirect role in the function of the protease. The examination of T80V and T80N indicates that Thr80 may not mutate to less chemically similar amino acids because of significant effects of protease activity. The catalytic efficiencies of T80S, T80V, and the WT were determined with a fluorescently labeled peptide substrate whose sequence is based on the MA-CA site of the HIV-1 protease (34). The catalytic efficiency of T80N versus this substrate could not be measured. While T80S had essentially WT activity, T80V only retained 6% of the WT protease's ability to cleave the MA-CA site. In order to examine the impact of these mutations at residue 80 on the virus as a whole, the SpIn of each variant was determined. As expected, the T80N virus was not infectious. However, the T80S virus and the T80V virus were within twofold of the infectiousness of the WT virus and had only slightly decreased processing of Gag relative to the WT virus. The discrepancy between the SpIn and catalytic efficiency results is likely due to the fact that the MA-CA cleavage is not the rate-determining step in viral maturation. Previous work with 14 fluorescently labeled peptide substrates of the HIV-1 protease determined that the catalytic efficiency of the WT protease cleaving the MA-CA site was 320-fold more efficient than the cleavage of the NC-p1 site (32). Mutations within the protease differentially impact the processing of the various substrates, and perhaps the Thr80Val mutation in the protease does not affect the rate-determining cleavage steps in viral maturation as dramatically as it affects the cleavage of the MA-CA site.

The role of residue 80 in the HIV-1 protease was further elucidated by examining a combination of crystal structures, MD simulations, and isothermal titration calorimetry. Through isothermal titration calorimetry, we found that the inhibitor SQV binds 2.3-fold more weakly to T80V than to the WT and 1,500-fold more weakly to T80N. In each case, the decrease in binding affinity is due to a much less favorable enthalpy of the interaction, which decreased by 5 and 17.7 kcal mol^{-1}, respectively, for T80V and T80N. This decrease possibly indicates a structural change in the bound state of protease between the variants, as seen in the crystal structure of T80N, where there was an obvious rearrangement of the residues in one of the P1 loops. The significantly less favorable enthalpy for both protease variants is partially compensated for by large favorable changes in the other component of the binding energy, entropy, with $\Delta(-T\Delta S)$ increases of -4.5 and -13.4 kcal mol^{-1} for T80V and T80N, respectively. One hypothesized reason for enthalpy-entropy compensation in other systems was a difference in the amount of bound water molecules from one variant to another that does not affect the overall binding affinity drastically but does affect the entropy-enthalpy balance (4, 5, 13, 59). While this may account for 1- to 2-kcal mol^{-1} changes in enthalpy and entropy, the huge entropy-enthalpy compensations observed in the case of T80V and T80N are probably due to a combination of effects.

In the case of the Thr80 variants, changes in thermodynamics are likely due to changes in the enzyme since the ligand,

SQV, and the solvent were constant between the reactions. For T80V, the mutation of polar threonine to hydrophobic valine could explain the observed changes in enthalpy and entropy. The loss of enthalpy in this case could be due to the inability of valine to form internal hydrogen bonds within the protease structure, while the increase in entropy could be due to the release of ordered waters solvating hydrophobic valine upon forming a complex with SQV. More ordered water would be needed to solvate hydrophobic valine than is needed to solvate the polar threonine; thus, more water would be released from the active site of T80V when binding SQV. Additionally, a valine would have more conformational freedom as it is not restricted by a hydrogen bond to the backbone. Both asparagine and threonine are polar residues, but asparagine is larger and capable of forming polar interactions with residues in the flap region. In the case of T80N, the -13.4-kcal mol^{-1} more favorable entropy could be due to the change in the flap dynamics that was observed in the MD simulation of the unliganded form of the enzyme. In contrast to the other protease variants, where the flaps are very flexible and a large loss of conformational entropy within the protease occurs upon forming a complex, the flaps of T80N are much less flexible. Therefore, there is less conformational entropy to lose with T80N and the binding would be entropically more favorable than with the other variants. Thus, combining the results of these biophysical measurements, the molecular role of Thr80 in the HIV-1 protease is that of a small hydrophilic residue that facilitates flap flexibility in the unliganded state while allowing tight packing of the active site in the liganded state of the enzyme. This mechanism may therefore account for the importance and observed invariance of Thr80 within the HIV-1 protease.

ACKNOWLEDGMENTS

REFERENCES

1. **Ala, P. J., E. E. Huston, R. M. Klabe, P. K. Jadhav, P. Y. Lam, and C. H. Chang.** 1998. Counteracting HIV-1 drug resistance: structural analysis of mutant proteases complexed with XV638 and SD146, cyclic urea amides with broad specificities. Biochemistry **37:**15042–15049.
2. **Ariyoshi, K., M. Matsuda, H. Miura, S. Tateishi, K. Yamada, and W. Sugiura.** 2003. Patterns of point mutations associated with antiretroviral drug treatment failure in CRF01_AE (subtype E) infection differ from subtype B infection. J. Acquir. Immune Defic. Syndr. **33:**336–342.
3. **Baldwin, E. T., T. N. Bhat, B. Liu, N. Pattabiraman, and J. W. Erickson.** 1995. Structural basis of drug resistance for the V82A mutant of HIV-1 proteinase. Nat. Struct. Biol. **2:**244–249.
4. **Beasley, J. R., D. F. Doyle, L. Chen, C. D. S., B. R. Fine, and G. J. Pielak.** 2002. Searching for quantitative entropy-enthalpy compensation among protein variants. Proteins Struct. Funct. Genet. **49:**398–402.
5. **Blasie, C. A., and J. M. Berg.** 2004. Entropy-enthalpy compensation in ionic interactions probed in a zinc finger peptide. Biochemistry **43:**10600–10604.
6. **Case, D. A., T. A. Darden, T. E. Cheatham III, C. L. Simmerling, J. Wang, R. E. Duke, R. Luo, K. M. Mertz, B. Wang, D. A. Pearlman, M. Crowley, S. Brozell, V. Tsui, H. Gohlke, J. Mongan, V. Hornak, G. Cui, P. Beroza, C. Schafmeister, J. W. Caldwell, W. S. Ross, and P. A. Kollman.** 2004. AMBER 8. University of California—San Francisco, San Francisco, Calif.
7. **Cheng, X., and T. A. Patterson.** 1992. Construction and use of λ P_L promoter vectors for direct cloning and high level expression of PCR amplified DNA coding sequences. Nucleic Acids Res. **20:**4591–4598.
8. **Chou, K.-C., A. G. Tomasselli, I. M. Reardon, and R. L. Heinrikson.** 1996. Predicting human immunodeficiency virus protease cleavage sites in proteins by a discriminant function method. Proteins **24:**51–72.
9. **Coffin, J. M.** 1995. HIV population dynamics in vivo: implications for genetic variation, pathogenesis and therapy. Science **257:**483–489.
10. **Collaborative Computational Project, Number 4.** 1994. The CCP4 suite: programs for protein crystallography. Acta Crystallogr. Sect. D Biol. Crystallogr. **50:**760–763.
11. **Copeland, R. A.** 1996. Enzymes: A practical introduction to structure, mechanism, and data analysis. Wiley-VCH, Weinheim, Germany.
12. **Cote, H. C. F., Z. L. Brumme, and P. R. Harrigan.** 2001. Human immunodeficiency virus type 1 protease cleavage site mutations associated with protease inhibitor cross-resistance selected by indinavir, ritonavir, and/or saquinavir. J. Virol. **75:**589–594.
13. **Dunitz, J. D.** 1995. Win some, lose some: enthalpy-entropy compensation in weak intermolecular interactions. Chem. Biol. **2:**709–712.
14. **Erickson, J. W., and S. K. Burt.** 1996. Structural mechanisms of HIV drug resistance. Annu. Rev. Pharmacol. Toxicol. **36:**545–571.
15. **Ermolieff, J., X. Lin, and J. Tang.** 1997. Kinetic properties of saquinavir-resistant mutants of human immunodeficiency virus type 1 protease and their implications in drug resistance in vivo. Biochemistry **36:**12364–12370.
16. **Ferrin, T. E., C. C. Huang, L. E. Jarvis, and R. Langridge.** 1988. The MIDAS display system. J. Mol. Graph. **6:**13–27.
17. **Gulnik, S. V., L. I. Suvorov, B. Liu, B. Yu, B. Anderson, H. Mitsuya, and J. W. Erickson.** 1995. Kinetic characterization and cross-resistance patterns of HIV-1 protease mutants selected under drug pressure. Biochemistry **34:**9282–9287.
18. **Henderson, L. E., T. D. Copeland, R. C. Sowder, A. M. Schultz, and S. Oraszlan.** 1988. Human retroviruses, cancer and AIDS: approaches to prevention and therapy. Liss, New York, N.Y.
19. **Hong, L., X. C. Zhang, J. A. Hartsuck, and J. Tang.** 2000. Crystal structure of an in vivo HIV-1 protease mutant in complex with saquinavir: insights into the mechanisms of drug resistance. Protein Sci. **9:**1898–1904.
20. **Hui, J. O., A. G. Tomasselli, I. M. Reardon, J. M. Lull, D. P. Brunner, C.-S. C. Tomich, and R. L. Heinrikson.** 1993. Large scale purification and refolding of HIV-1 protease from Escherichia coli inclusion bodies. J. Protein Chem. **12:**323–327.
21. **Ji, J. P., and L. A. Loeb.** 1992. Fidelity of HIV-1 reverse transcriptase copying RNA in vitro. Biochemistry **31:**954–958.
22. **Jones, T. A., M. Bergdoll, and M. Kjeldgaard.** 1990. O: a macromolecular modeling environment, p. 189–195. In C. Bugg and S. Ealick (ed.), Crystallographic and modeling methods in molecular design. Springer-Verlag, Berlin, Germany.
23. **Kantor, R., and D. Katzenstein.** 2004. Drug resistance in non-subtype B HIV-1. J. Clin. Virol. **29:**152–159.
24. **Kantor, R., R. W. Shafer, S. Follansbee, J. Taylor, D. Shilane, L. Hurley, D. P. Nguyen, D. Katzenstein, and W. J. Fessel.** 2004. Evolution of resistance to drugs in HIV-1-infected patients failing antiretroviral therapy. AIDS **18:**1503–1511.
25. **King, N. M., L. Melnick, M. Prabu-Jeyabalan, E. A. Nalivaika, S.-S. Yang, Y. Gao, X. Nie, C. Zepp, D. L. Heefner, and C. A. Schiffer.** 2002. Lack of synergy for inhibitors targeting a multi-drug-resistant HIV-1 protease. Protein Sci. **11:**418–429.
26. **King, N. M., M. Prabu-Jeyabalan, P. Wigerinck, M.-P. De Bethune, and C. A. Schiffer.** 2004. Structural and thermodynamic basis for the binding of TMC114, a next-generation human immunodeficiency virus type 1 protease inhibitor. J. Virol. **78:**12012–12021.
27. **Klabe, R. M., L. T. Bacheler, P. J. Ala, S. Erickson-Viitanen, and J. L. Meek.** 1998. Resistance to HIV protease inhibitors: a comparison of enzyme inhibition and antiviral potency. Biochemistry **37:**8735–8742.
28. **Kohl, N. E., E. A. Emini, W. A. Schleif, L. J. Davis, J. C. Heimbach, R. A. Dixon, E. M. Scolnick, and I. S. Sigal.** 1988. Active human immunodeficiency virus protease is required for viral infectivity. Proc. Natl. Acad. Sci. USA **85:**4686–4690.
29. **Krohn, A., S. Redshaw, J. C. Ritchie, B. J. Graves, and M. H. Hatada.** 1991. Novel binding mode of highly potent HIV-proteinase inhibitors incorporating the (R)-hydroxyethylamine isostere. J. Med. Chem. **34:**3340–3342.
30. **Kuriyan, J., and W. I. Weis.** 1991. Rigid protein motion as a model for crystallographic temperature factors. Proc. Natl. Acad. Sci. USA **88:**2773–2777.
31. **Laskowski, R. A., M. W. Mac Arthur, D. S. Moss, and J. M. Thornton.** 1993. PROCHECK. A program to check the stereochemical quality of protein structures. J. Appl. Crystallogr. **26:**283–291.
32. **Maguire, M. F., R. Guinea, P. Griffin, S. MacManus, R. C. Elston, J. Wolfram, N. Richards, M. H. Hanlon, D. J. T. Porter, T. Wrin, N. Parkin, M. Tisdale, E. S. Furfine, C. Petropoulos, B. W. Snowden, and J. P. Kleim.** 2002. Changes in human immunodeficiency virus type 1 Gag at positions L449 and P453 are linked to I50V protease mutants in vivo and cause reduction of

sensitivity to amprenavir and improved viral fitness in vitro. J. Virol. **76:** 7398–7406.

33. **Maschera, B., G. Darby, G. Palu, L. L. Wright, M. Tisdale, R. Myers, E. D. Blair, and E. S. Furfine.** 1996. Human immunodeficiency virus: mutations in the viral protease that confer resistance to saquinavir increase the dissociation rate constant of the protease-saquinavir complex. J. Biol. Chem. **271:** 33231–33235.

34. **Matayoshi, E., G. Wang, G. Krafft, and J. Erickson.** 1990. Novel fluorogenic substrates for assaying retroviral proteases by resonance energy transfer. Science **247:**954–958.

35. **Minor, W.** 1993. XDISPLAYF program. Purdue University, West Lafayette, Ind.

36. **Morris, R. J., A. Perrakis, and V. S. Lamzin.** 2002. ARP/wARP's model-building algorithms. I. The main chain. Acta Crystallogr. Sect. D Biol. Crystallogr. **58:**968–975.

37. **Munshi, S., Z. Chen, Y. Yan, Y. Li, D. Olsen, H. Schock, B. Galvin, B. Dorsey, and L. Kuo.** 2000. An alternate binding site for the P1-P3 group of a class of potent HIV-1 protease inhibitors as a result of concerted structural change in the 80s loop of the protease. Acta Crystallogr. Sect. D Biol. Crystallogr. **56**(Pt. 4)**:**381–388.

38. **Murshudov, G. N., A. A. Vagin, and E. J. Dodson.** 1997. Refinement of macromolecular structures by the maximum-likelihood method. Acta Crystallogr. Sect. D Biol. Crystallogr. **53:**240–255.

39. **Muzammil, S., P. Ross, and E. Freire.** 2003. A major role for a set of non-active site mutations in the development of HIV-1 protease drug resistance. Biochemistry **42:**631–638.

40. **Navaza, J.** 1994. AMoRe: an automated package for molecular replacement. Acta Crystallogr. Sect. A **50:**157–163.

41. **Ohtaka, H., A. Schon, and E. Freire.** 2003. Multidrug resistance to HIV-1 protease inhibition requires cooperative coupling between distal mutations. Biochemistry **42:**13659–13666.

42. **Ohtaka, H., A. Velazquez-Campoy, D. Xie, and E. Freire.** 2002. Overcoming drug resistance in HIV-1 chemotherapy: the binding thermodynamics of amprenavir and TMC-126 to wild-type and drug-resistant mutants of the HIV-1 protease. Protein Sci. **11:**1908–1916.

43. **Otwinowski, Z., and W. Minor.** 1997. Processing of X-ray diffraction data collected in oscillation mode. Methods Enzymol. **276:**307–326.

44. **Pettit, S. C., G. J. Henderson, C. A. Schiffer, and R. Swanstrom.** 2002. Replacement of the P1 amino acid of human immunodeficiency virus type 1 Gag processing sites can inhibit or enhance the rate of cleavage by the viral protease. J. Virol. **76:**10226–10233.

45. **Pettit, S. C., N. Sheng, R. Tritch, S. Erickson-Vitanen, and R. Swanstrom.** 1998. The regulation of sequential processing of HIV-1 Gag by the viral protease. Adv. Exp. Med. Biol. **436:**15–25.

46. **Prabu-Jeyabalan, M., E. Nalivaika, N. M. King, and C. A. Schiffer.** 2004. Structural basis for coevolution of the human immunodeficiency virus type 1 nucleocapsid-p1 cleavage site with a V82A drug-resistant mutation in viral protease. J. Virol. **78:**12446–12454.

47. **Prabu-Jeyabalan, M., E. Nalivaika, and C. A. Schiffer.** 2000. How does a symmetric dimer recognize an asymmetric substrate? A substrate complex of HIV-1 protease. J. Mol. Biol. **301:**1207–1220.

48. **Prabu-Jeyabalan, M., E. A. Nalivaika, N. M. King, and C. A. Schiffer.** 2003.

49. **Resch, W., R. Ziermann, N. Parkin, A. Gamarnik, and R. Swanstrom.** 2002. Nelfinavir-resistant, amprenavir-hypersusceptible strains of human immunodeficiency virus type 1 carrying an N88S mutation in protease have reduced infectivity, reduced replication capacity, and reduced fitness and process the Gag polyprotein precursor aberrantly. J. Virol. **76:**8659–8666.

50. **Roberts, J. D., K. Bebenek, and T. A. Kunkel.** 1988. The accuracy of reverse transcriptase from HIV-1. Science **242:**1171–1173.

51. **Roberts, J. D., B. D. Preston, L. A. Johnston, et al.** 1989. Fidelity of two retroviral reverse transcriptases during DNA-dependent DNA synthesis in vitro. Mol. Cell. Biol. **9:**469–476.

52. **Roberts, N. A.** 1995. Drug-resistance patterns of saquinavir and other HIV proteinase inhibitors. AIDS **9**(Suppl. 2)**:**S27–S32.

53. **Robins, T., and J. Plattner.** 1993. HIV protease inhibitors: their anti-HIV activity and potential role in treatment. J. Acquir. Immune Defic. Syndr. **6:**162–170.

54. **Rose, J. R., R. Salto, and C. S. Craik.** 1993. Regulation of autoproteolysis of the HIV-1 and HIV-2 proteases with engineered amino acid substitutions. J. Biol. Chem. **268:**11939–11945.

55. **Schinazi, R. F., B. A. Larder, and J. W. Mellors.** 1997. Mutations in retroviral genes associated with drug resistance. Int. Antiviral News **5:**129–142.

56. **Schomaker, V., and K. N. Trueblood.** 1968. On the rigid body motion of molecules in crystals. Acta Crystallogr. Sect. B **24:**63–76.

57. **Scott, W. R. P., and C. A. Schiffer.** 2000. Curling of flap tips in HIV-1 protease as a mechanism for substrate entry and tolerance of drug resistance. Structure **8:**1259–1265.

58. **Shafer, R. W., D. Stevenson, and B. Chan.** 1999. Human immunodeficiency virus reverse transcriptase and protease sequence database. Nucleic Acids Res. **27:**348–352.

59. **Sharp, K.** 2001. Enthalpy-entropy compensation: fact or artifact? Protein Sci. **10:**661–667.

60. **Sigurskjold, B.** 2000. Exact analysis of competition ligand binding by displacement isothermal titration calorimetry. Anal. Biochem. **277:**260–266.

61. **Tickle, I. J., and D. S. Moss.** 1999. Modelling rigid-body thermal motion in macromolecular crystal structure refinement. IUCr99 Computing School, London, United Kingdom. [Online.] http://people.cryst.bbk.ac.uk/~tickle /iucr99/.

62. **Todd, M. J., I. Luque, A. Velazquez-Campoy, and E. Freire.** 2000. Thermodynamic basis of resistance to HIV-1 protease inhibition: calorimetric analysis of the V82F/I84V active site resistant mutant. Biochemistry **39:**11876–11883.

63. **Tözsér, J., I. Blaha, T. D. Copeland, E. M. Wondrak, and S. Oroszlan.** 1991. Comparison of the HIV-1 and HIV-2 proteinases using oligopeptide substrate representing cleavage sites in Gag and Gag-Pol polyproteins. FEBS Lett. **281:**77–80.

64. **Velazquez-Campoy, A., Y. Kiso, and E. Freire.** 2001. The binding energetics of first- and second-generation HIV-1 protease inhibitors: implications for drug design. Arch. Biochem. Biophys. **390:**169–175.

65. **Xie, D., S. Gulnik, E. Gustchina, B. Yu, W. Shao, W. Qoronfleh, A. Nathan, and J. W. Erickson.** 1999. Drug resistance mutations can effect dimer stability of HIV-1 protease at neutral pH. Protein Sci. **8:**1702–1707.

Viability of a drug-resistant HIV-1 protease variant: structural insights for better antiviral therapy. J. Virol. **77:**1306–1315.